

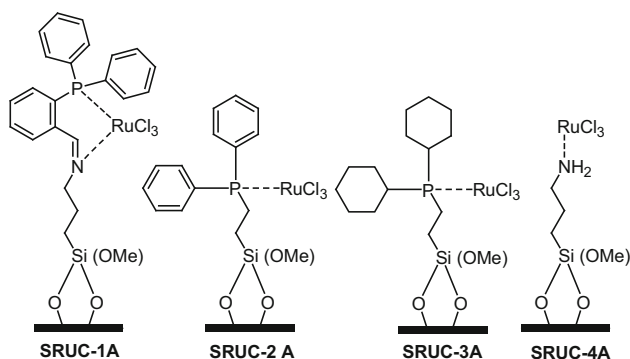
# Heterogeneous Silica Tethered Ruthenium Catalysts for Carbon Sequestration Reaction

Praveenkumar Ramprakash Upadhyay<sup>1</sup> · Vivek Srivastava<sup>1</sup>

Received: 26 April 2016 / Accepted: 17 May 2016 / Published online: 2 June 2016  
© Springer Science+Business Media New York 2016

**Abstract** A series of silica-tethered Ru complexes were easily prepared and further analyzed by sophisticated analytical techniques such as FTIR, N<sub>2</sub> physisorption, ICP-OES and XPS analysis. After proper characterization of catalyst structure, we exploited them to synthesize formic acid followed by CO<sub>2</sub> hydrogenation reaction. To determine the exact amount of reaction product (formic acid) in the reaction mixture we performed the <sup>1</sup>H NMR analysis, using dioxane as an internal standard. No degradation of dioxane as well as the side product formation was recorded in this study. Reported catalytic systems were found active and stable in terms of formic acid formation and catalyst recycling experiment up to nine consecutive runs.

## Graphical Abstract



**Keywords** Silica · Ru complex · Formic acid · Carbon dioxide · Carbon sequestration

## 1 Introduction

Carbon dioxide (CO<sub>2</sub>) gas has become a great global interest from, both practical and theoretical point of view as CO<sub>2</sub> is the major backer to the greenhouse effect [1–3]. In recent years, CO<sub>2</sub> exploitation and its conversion into the value added chemicals have fascinated great consideration of leading research groups [4–6]. Although, CO<sub>2</sub> is extensively acknowledged as a reactant for the synthesis of carbonates and other vital chemicals such as methanol, aspirin, formic acid etc., but CO<sub>2</sub> reduction is still hurting because of its extreme thermodynamic stability. In the view of exceptional stability of CO<sub>2</sub>, it's a major challenge to develop new competent and highly reductive protocol to make them ready for chemical reaction under mild reaction condition [7–9]. Catalytic hydrogenation of CO<sub>2</sub> gas has become as a useful method to fix CO<sub>2</sub> either in chemicals or chemical intermediates [10–12].

Formic acid is considered as a significant chemical feedstock for the number of chemical industries such as perfume, dyeing and sanitary industry (as disinfectant and preservatives) [10, 11, 13–16]. Apart from above mentioned applications of formic acid, it also applied in the production format ester, which further utilized for the synthesis of aldehydes, ketones, amides and carboxylic acid [13–16]. The commercial process of formic acid synthesis is based on the hydrolysis of methyl format [17, 18] or by the reaction of CO with water [19]. All these conventional approaches agonize with producing perilous waste and consume heavy volumes of electricity because of

✉ Vivek Srivastava  
vivek.shrivastava@niituniversity.in

<sup>1</sup> Basic Sciences, NIIT University, HN-8 Delhi-Jaipur Highway, Neemrana, Rajasthan, India

that it's a necessity to develop more environmentally clean process for the production of formic acid [14–16].

A range of unsupported, homogenous transition metal catalysts such as Ru, Rh, Ir and Pt (as hail or hybrids) to efficiently catalyze the CO<sub>2</sub> hydrogenation reaction [10, 19–21]. Surprisingly, very few reports are available on tethered heterogeneous catalysts for the hydrogenation of CO<sub>2</sub> gas. Organic–inorganic hybrid catalysts are the promising class of tethered heterogeneous catalysts, are designed to retain the selectivity of homogeneous catalysts while being immobilized them on heterogeneous support to obtain easy separation [19]. However, very few reports have represented the applications of tethered heterogeneous catalysts for the reduction of CO<sub>2</sub> gas. Baiker and co-authors reported co-condensation method to incorporate a transition metal complex based on Ru, Ir, Pt, or Pd within a silica support [21]. As per report, Ru-phosphine hybrid catalysts gave best catalytic activity to synthesize *N,N*-diethylformamide from CO<sub>2</sub>, H<sub>2</sub>, and diethylamine. Aminosilicate-tethered Ru complex was reported by Yu and co-authors for hydrogenation of CO<sub>2</sub> to formic acid with the TON value of 1482 h<sup>-1</sup> [22]. To achieve this TON value they used PPh<sub>3</sub> with supercritical CO<sub>2</sub> at 80 °C. In another report, Hicks and Jones reported the synthesis of a series of silica tethered iridium catalyst for the CO<sub>2</sub> hydrogenation reaction. The achieve the formic acid as a reaction product with good TON value (27 × 10<sup>2</sup> h<sup>-1</sup>) at 60 °C after 20 h of reaction [23, 24]. Although, mentioned catalytic systems were found effective for CO<sub>2</sub> hydrogenation, but these systems also suffered in terms of long reaction time, high catalyst loading and catalyst recycling.

In this report, we are offering the synthesis of silica-tethered ruthenium catalyst (SRUC) for the hydrogenation of CO<sub>2</sub> to formic acid. The SRUC catalytic system was synthesized by a multistep grafting process using iminophosphine ligand tethered to mesoporous SBA-15 inorganic support. After activating the SRUC catalyst with hydrogen gas, it was applied as hydrogenating catalyst for CO<sub>2</sub> gas.

## 2 Experimental

Reagent Plus<sup>®</sup> grade chemicals were purchased from Sigma Aldrich and other suppliers. All the Nuclear Magnetic Resonance (NMR) (<sup>1</sup>H/<sup>13</sup>C/<sup>31</sup>P) spectra were recorded on a standard Bruker 300WB spectrometer with an Avance console at 400 and 100 MHz. The FTIR measurements were conducted with a Bruker Tensor 27 in DRIFTS mode (KBr powder) with a scan range from 400 to 4000 cm<sup>-1</sup>. All the hydrogenation reactions were carried out in a 100 mL stainless steel autoclave (Amar Equipment, India). Energy-dispersive FTIR data for all the samples were studied with Bruker Tensor-27. Elemental

analysis was conducted in a Perkin Elmer Optima 3300 XL ICP-OES to determine the metal Ru and P content. BET surface area, pore size, and pore volume measurements of the catalysts were determined from a physical adsorption of N<sub>2</sub> using liquid nitrogen by an ASAP2420 Micromeritics adsorption analyzer (Micromeritics Instruments Inc.). The metal contents in the heterogeneous catalysts were determined by using EDX, Quantax 200 Energy Dispersive X-ray Spectrometer. Scanning electron microscopy (SEM) images of support and catalyst were measured on SEM, JEOL JSM-840 A.

### 2.1 Synthesis of SBA-15 [23]

Poly(ethylene glycol)-blockpoly(propylene glycol)-blockpoly (ethylene glycol) (P-123) (15 g) was allowed to react with distilled water (650 g) and concentrated HCl (80 g) for 3 h. Afterward, tetraethyl orthosilicate (TEOS) (35 g) was added to the above micellar solution and the total reaction mass was stirred for 30 h at 40 °C in oven. To achieve proper swelling pores and aging, the same reaction mass was heated at 80 °C for another 24 h. Several washings were used (by distilled water) to obtain resulting solid. Further, solid material was kept under vacuum drying at 50 °C for 12 h. The process of calcination was carried out at 550 °C for 7 h with a temperature ramp of 1.2 °C/min. The pretreatment was carried out before using the SBA-15, and it was vacuum dried at 200 °C for 3 h (82 % yield). The SBA-15 was kept in an N<sub>2</sub> atmosphere for storage.

### 2.2 Synthesis of Iminophosphine Ligand Without Alkoxy silane Moiety A [25]

A Schiff–base reaction carried out under nitrogen atmosphere by adding 2-(diphenylphosphino)benzaldehyde (2.1 mmol) and 1-Propylamine (10 mL) in reaction appropriate vessel. The resulting reaction mixture was refluxed for 5 h. After cooling the reaction mass up to room temperature the red, brown oil was obtained by removing the unutilized 1-propylamine under high pressure vacuum (89 % yield).

<sup>1</sup>H NMR (400 MHz, CD<sub>2</sub>Cl<sub>2</sub>): δ = 9.01 (s, 1H), 8.03 (s, 1H), 7.45–7.29 (m, 12 H), 6.98 (s, 1 H), 3.43 (t, 2 H), 1.57–1.52 (q, 2 H), 0.82–0.78 (t, 3 H); <sup>13</sup>C NMR (100 MHz, CD<sub>2</sub>Cl<sub>2</sub>): δ = 160.01, 134.24, 128.74, 63.33, 23.95, 11.78 ppm; <sup>31</sup>P NMR: (300 MHz, CD<sub>2</sub>Cl<sub>2</sub>, ppm) δ = -13.01 ppm.

### 2.3 Synthesis of Alkoxy silane-Containing Bidentate Iminophosphine Ligand Moiety B

The synthesis of the iminophosphine ligand carrying alkoxy silane moiety A was performed through the reactive

distillation of 2-(diphenylphosphino)benzaldehyde (0.500 g) with 3-(aminopropyl)trimethoxysilane (0.250 g) in dry toluene (25 mL). After 5 h, we obtained a yellow oily liquid by careful removal of toluene under vacuum (85 % yield).

$^1\text{H}$  NMR (400 MHz,  $\text{CD}_2\text{Cl}_2$ ):  $\delta$  = 8.8 (s, 1H), 8.02 (s, 1H), 7.45–7.27 (m, 12 H), 6.91 (s, 1 H), 3.53 (s, 9 H), 3.46 (m, 2 H), 1.68–1.60 (m, 2 H), 0.58–0.52 (m, 2 H);  $^{13}\text{C}$  NMR (100 MHz,  $\text{CD}_2\text{Cl}_2$ ):  $\delta$  = 158.57, 134.14, 128.79, 65.13, 50.82, 24.62, 8.73 ppm;  $^{31}\text{P}$  NMR: (300 MHz,  $\text{CD}_2\text{Cl}_2$ , ppm)  $\delta$  = –13.07 ppm.

#### 2.4 Synthesis of Phosphine-Functionalized SBA-15 (IPPL-SBA-15 1A-3A) [24, 26, 27]

Post-synthetic grafting technique was used to obtain phosphine functionalized SBA-15 under a nitrogen atmosphere. Phosphine ligand (2.1 mmol) was added to the dry SBA-15 powder (1 g) in dry toluene (25 mL) under  $\text{N}_2$ . The reaction mass was stirred for next 20 h at room temperature (25–30 °C). The resulting solid was washed with anhydrous toluene ( $10 \times 2$  mL). The recovered solid was carefully dried under vacuum at room temperature and stored in nitrogen atmosphere (87 % yield).

#### 2.5 Synthesis of Amine-Functionalized SBA-15 (IPPL-SBA-15 4A) [25]

3-Aminopropyltrimethoxysilane (1.15 g) was added to the dried SBA-15 powder (1 g) in toluene (50 mL) under  $\text{N}_2$  atmosphere. The combined reaction mass was allowed to stir for 24 h at room temperature (20–30 °C) under  $\text{N}_2$  atmosphere. The subsequent solid was washed and filtered with anhydrous toluene ( $10 \times 2$  mL) and dried under vacuum at 80 °C. The final product was stored in a nitrogen gas (85 % yield).

#### 2.6 Synthesis of Ru-Tethered Pre-catalysts (SURC 1A-4A)

The reaction was carried out by refluxing in anhydrous ethanol with  $\text{RuCl}_3 \cdot 3\text{H}_2\text{O}$  under nitrogen atmosphere for 12 h. The Ru/P molar ratio was maintained to 1/1. The resulting reaction mixture was degassed and kept under nitrogen atmosphere. The cleaning of material was carried out carefully with anhydrous ethanol in the presence of  $\text{N}_2$  gas. The recovered solid was then dried under vacuum at room temperature for 24 h, lastly warehoused in the  $\text{N}_2$  atmosphere (91 % yield).

### 3 Synthesis of Ru Complex with Iminophosphine Ligand (Ru-Moiety A)

The reaction vessel was charged with moiety A (2.0 g),  $\text{RuCl}_3 \cdot 3\text{H}_2\text{O}$  (2.10 g) and dry ethanol (25 mL). The reaction mass was allowed to reflux under Argon atmosphere 10 h. The resulting reaction mixture was filtered and then with dry ethanol. All the process was completed under argon atmosphere. The material (98.5 % yield) was dried and stored under argon atmosphere.

#### 3.1 $\text{CO}_2$ Hydrogenation Reaction and Catalyst Recycling [28, 29]

The high pressure autoclave (100 mL) was charged with catalyst, triethylamine (2 mL) and water (as per requirement). In a typical reaction, a 150  $\mu\text{M}$  catalyst concentration was loaded in autoclave. A known amount of dioxane was added with reactants (as an internal standard), to quantify the reaction kinetics with  $^1\text{H}$  NMR spectroscopy. It is important to notify that no decomposition of dioxane was found under all reaction conditions. After careful addition of all the required reactants, the air of reaction vessel was replaced with nitrogen gas (*five times nitrogen purging was carried out*). Then the catalyst activation step was done at 20 bar hydrogen pressure for 20 min at 35 °C. Nitrogen gas was used to replace all the gasses after completion of catalyst activation step. Then only, the reaction vessel was charged with  $\text{CO}_2$  and  $\text{H}_2$  gas (desired quantity) by replacing the nitrogen gas and the total reaction mass was allowed to stir for next 2 h at 100 °C. After cooling the reaction mass using ice cold water (2–5 °C), gas pressure was released. A small amount of crude reaction mass was used for  $^1\text{H}$  NMR analysis. Water was evaporated from the reaction mass at 110 °C, and then formic acid was isolated from the reaction mass with the help of nitrogen gas flow at 125–130 °C, passing through the water trap, in order to capture formic acid [28, 29]. Acid base titration was used to calculate the amount formic acid in water trap. The results obtained from  $^1\text{H}$  NMR analysis as well as from titration method were found in good agreement to each other.

In recycling experiment, catalytic system was washed with dry diethyl ether ( $5 \times 2$  mL) and kept under vacuum 12 h at 40 °C (all the product isolation steps as well as catalyst cleaning steps were carried out in the autoclave to avoid the catalyst loss). Then, the catalytic system went for recycling experiment where, recovered catalyst was allowed to stir under nitrogen atmosphere (2 bar) for 1 h at room temperature. Later, nitrogen was replaced by hydrogen gas and reaction mass was stirred under hydrogen

atmosphere (4 bar) for 20 min at 35 °C. Then only, all the steps were completed as per above mentioned CO<sub>2</sub> hydrogenation protocol.

## 4 Result and Discussion

### 4.1 Synthesis and Characterization of Catalysts

In this report, we are offering the synthesis of SRUC for the hydrogenation of CO<sub>2</sub> gas to formic acid. The SRUC catalytic system was synthesized by a multistep grafting process using iminophosphine ligand tethered to mesoporous SBA-15 inorganic support. After activating the SRUC catalyst with hydrogen gas, it was applied as hydrogenating catalyst for CO<sub>2</sub> gas. It is worth noted that, SBA-15 was synthesized as per reported protocol and the important IV-type isotherm was recorded while performing N<sub>2</sub> physisorption analysis. The acceptable BET surface area (950 m<sup>2</sup>/g) and Barrett–Joyner–Halenda pore size (6.1 nm) was recorded for synthesized SBA-15. The alkoxy-silane-containing bidentate imonophosphine ligand [*o*-Ph<sub>2</sub>PC<sub>6</sub>H<sub>4</sub>CH=N(CH<sub>2</sub>)<sub>3</sub>Si(OMe)<sub>3</sub>] **A** was obtained as per previously reported procedure by reacting *o*-(diphenylphosphino)benzaldehyde with 3-(aminopropyl)trimethoxysilane under nitrogen atmosphere in dry toluene solvent system (Schiff–base reaction) [24–27]. All the NMR (<sup>1</sup>H/<sup>13</sup>C/<sup>31</sup>P) data were found in good agreement with previously published reports [24–27]. In the next step, imonophosphine ligand **A** was sensibly grafted on well characterized SBA-15 to get **IPPL-SBA-15 1A** (Fig. 1). Then finally, **IPPL-SBA-15 1A** went to metallation steps, where **IPPL-SBA-15 1A** was allowed to reflux with hydrated RuCl<sub>3</sub> in dry ethanol. The resulting **SRUC-1A**

was obtained in black color and wisely stored in nitrogen atmosphere. Some more monodentate phosphine pre-catalysts such as **SRUC-2A**, **SRUC-3A** and **SRUC-4A** (primary amine pre-catalyst) (Fig. 2) were created along with **IPPL-SBA-15 2A**, **IPPL-SBA-15 3A** and **IPPL-SBA-15 4A** materials respectively to go for proper comparative study. Iminophosphine ligand without alkoxy-silane moiety **B** was also synthesized to go for relative study of hybrid materials.

Sophisticated and important analytical techniques were applied to understand the physiochemical properties of the SRUC (**SRUC-1A**, **SRUC-2A**, **SRUC-3A** and **SRUC-4A**) such as FTIR, XPS, SEM–EDS, N<sub>2</sub> physisorption and inductively coupled plasma optical emission spectroscopy (ICP-OES).

In DRIFT spectra, while comparing the recorded data of iminophosphine ligand without alkoxy-silane moiety **A** (Ru(Cl<sub>3</sub>)Ph<sub>2</sub>PC<sub>6</sub>H<sub>4</sub>CH=N(CH<sub>2</sub>)<sub>2</sub>CH<sub>3</sub>) and moiety **B** iminophosphine Ligand (Ph<sub>2</sub>PC<sub>6</sub>H<sub>4</sub>CH=N(CH<sub>2</sub>)<sub>2</sub>CH<sub>3</sub>) with **SRUC 1A-4A**, the Schiff base (CH=NR) double-bond adsorption appears at 1640 cm<sup>-1</sup>, while phenyl ring vibration caught near 3062, 1585, 1431, 742, and 695 cm<sup>-1</sup>. Same absorption peaks were again recorded for tethered materials **IPPL-SBA-15 1A** and **SRUC-1A**. These data reflected the presence of Schiff base before and after the metallation. The monodentate phosphine pre-catalysts **SRUC-2A**, **3A** and **4A** gave different absorption data in there FTIR analysis (Figs. 3, 4, 5).

Before going to the metallation step, N<sub>2</sub>-physisorption analysis was carried out for SBA-15 and bifunctional ligands modified SBA-15. All the recovered data were summarized in Table 1, where with respect to SBA-15 the pore size was reduced after modifying it to bifunctional ligands.

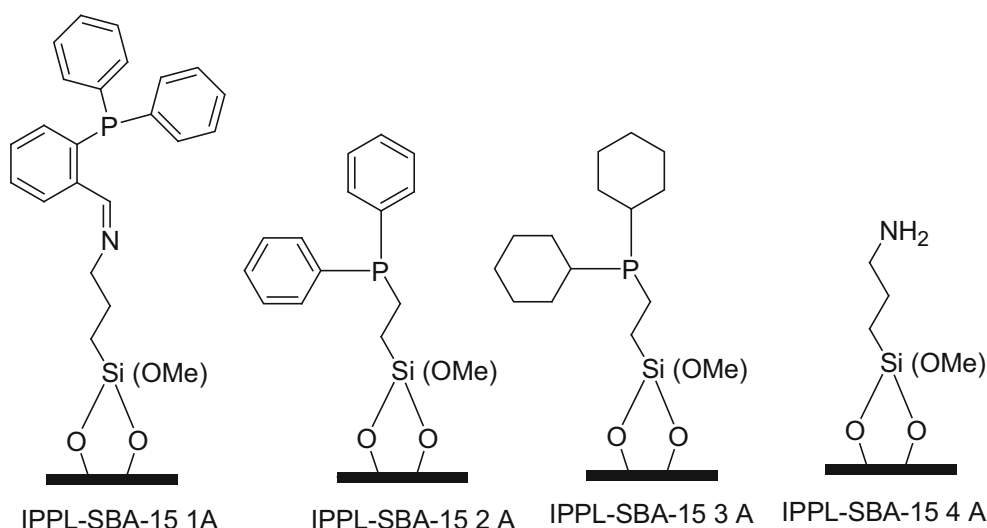


**Fig. 1** Structure of SBA-15 tethered phosphine ligands

**Fig. 2** SBA-15 tethered ruthenium catalysts

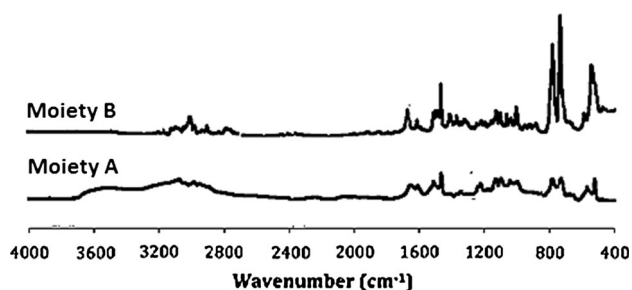
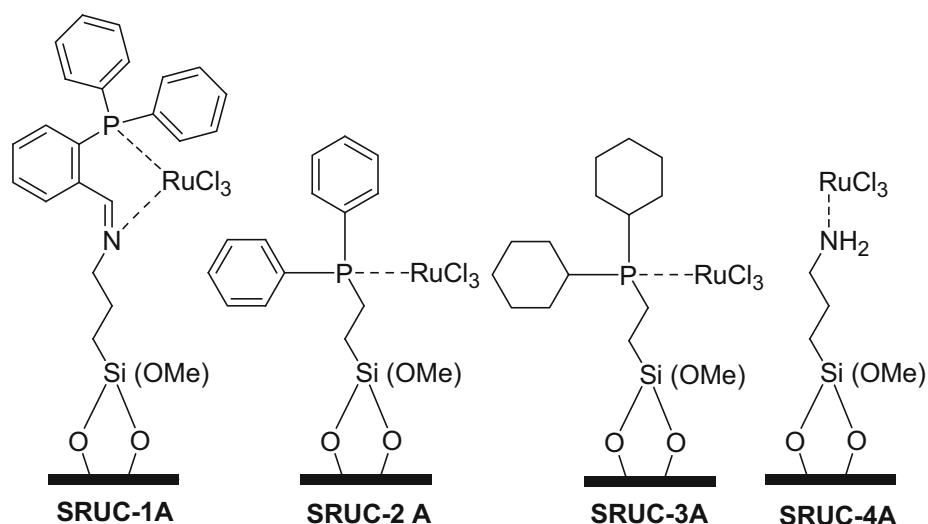


**Fig. 3** FTIR spectra of unsupported moiety 1 and 2

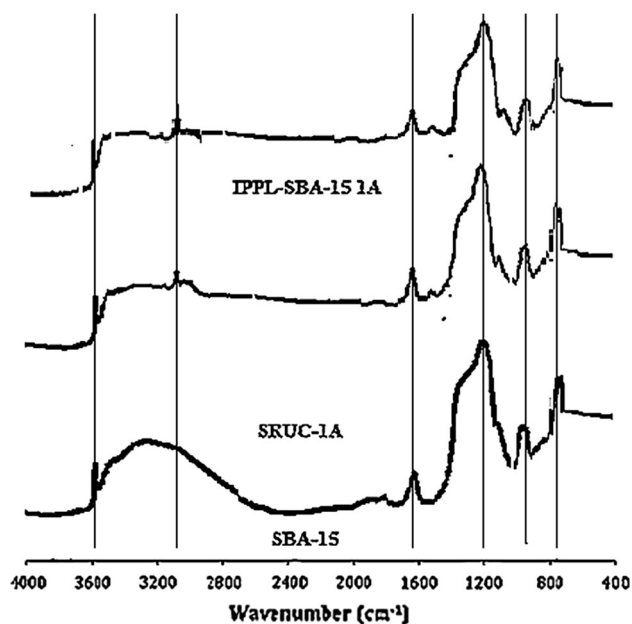


**Fig. 4** DRIFT data for SURC-1A and IPPL-SBA-15 1A with respect to SBA-15

To understand the composition of synthesized materials, we performed XPS analysis. In XPS spectra Ru 3d, C 1s, N 1s and P 2p levels were measured at a normal angle with respect to the plane of the surface. High-resolution spectra were corrected for charging effects by assigning a value of 284.6 eV to the C 1s peak (adventitious carbon). Binding energies were determined with an accuracy of  $\pm 0.2$  eV. Synthetic components on Ru 3d–C 1s were analyzed with a Shirley background subtraction and a peak shape with a combination of Gaussian and Lorentzian (30 % Lorentzian). The peaks at 280.2 (Ru 3d<sub>5/2</sub>) and 284.3 eV (Ru 3d<sub>3/2</sub>) were confirmed the presence of Ru (0) [20]. Surprisingly, in XPS study no peaks were recorded near to 281.1 and 287.1 eV, which confirmed the absence of Ru<sub>2</sub>O species. Also, no Ru 3p core level peak with a binding energy of 464 eV was noted for the neat **SRUC 1–4A** samples. This observation also confirmed the absence of ruthenium in +2 oxidation state.

As shown in Table 2, XPS analysis of supported RuCl<sub>3</sub>/SBA-15 exhibited a low binding energy of Ru 3d<sub>3/2</sub> and 3d<sub>5/2</sub> confirmed the presence of Ru (0) species relative to the binding energies of **SRUC-1A** and **SRUC-3A**. Surprisingly, there is some resemblance in the Ru 3d<sub>3/2</sub> and 3d<sub>5/2</sub> binding energies between **SRUC-2A** and RuCl<sub>3</sub>/SBA-15, which could be the result relatively low loading of the phosphine ligand on the support (Fig. 6). This would allow RuCl<sub>3</sub> to interact with residual silanol groups on the support (Fig. 6). In opposite, **SRUC-3A** gave much higher loading of the anchored phosphine, which resulted in a higher binding energy for Ru 3d<sub>3/2</sub> and 3d<sub>5/2</sub>. Furthermore, **SRUC-1A** had slightly higher binding energy for 3d<sub>3/2</sub> and 3d<sub>5/2</sub> than **SRUC-3A**. Interestingly, the shift in the 3d<sub>3/2</sub> and 3d<sub>5/2</sub> peak of the unsupported analogue was 284.7 eV (Ru-PNPr<sup>1</sup>), which was similar to **SRUC-1A**. These results

indicate that the environment of Ru in the tethered bidentate material is perhaps comparable to that in the unsupported Ru-PNPr<sup>1</sup> analogue. SEM-EDX spectrum of

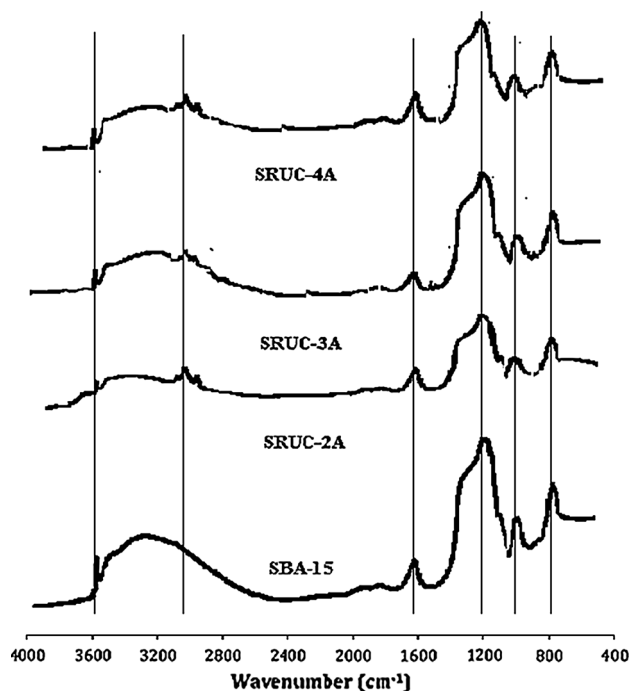


Fig. 5 DRIFT data for SURC-1A-4A with respect to SBA-15

**Table 1** Physical properties of SBA-15 modified materials

Materials	$S_{\text{BET}}$ (m <sup>2</sup> /g)	Pore volume (cm <sup>3</sup> /g)	Pore size (nm)
IPPL-SBA-15 1A	688	0.74	5.9
IPPL-SBA-15 2A	271	0.36	4.0
IPPL-SBA-15 3A	419	0.51	4.9
IPPL-SBA-15 4A	365	0.46	5.0
SBA-15	950	0.85	6.1

**Table 2** XPS analysis of developed materials

Samples	Ru 3d <sub>3/2</sub> (eV)	Ru 3d <sub>5/2</sub> (eV)	Cl <sub>2</sub> 2p (eV)	P 2p (eV)	N 1s (eV)
RuCl <sub>3</sub>	284.6	280.2	199.2	–	–
RuCl <sub>3</sub> /SBA-15	284.4	280.1	199.1	–	–
Ru-PNPr <sup>1</sup>	284.7	280.8	198.6	131.9	399.8
IPPL-SBA-15 1A	–	–	–	131.8	398.1
IPPL-SBA-15 2A	–	–	–	–	–
IPPL-SBA-15 3A	–	–	–	131.1	–
IPPL-SBA-15 4A	–	–	–	131.1	–
SRUC-1A	284.7	280.8	197.1	131.8-	400.1-
SRUC-2A	284.7	284.8	198.6	131.7	–
SRUC-3A	284.6	284.5	199.3	131.6	–
SRUC-4A	284.6	284.5	199.3	–	400.2-
SRUC-2A	284.6	284.4	198.5	131.6	–

(after catalyst recycling)

Measurement error of  $\pm 0.2$  eV; XPS data of Si 2p at 103.3 eV. XPS data referenced to C 1s at 284.5 eV

SRUC-1A with respect to IPPL-SBA-15 1A further confirmed the presence of Ru in the SRUC-1A (Fig. 6).

ICP-OES and TGA analysis were carried out to calculate the loading of phosphine on SBA-15 as well as ligand loading on SBA-15 respectively (Fig. 7). Maximum phosphine piling was recorded in IPPL-SBA-15 2A and the lowest loading was noted with IPPL-SBA-15 1A. This observation was also found in good agreement with XPS analysis. Higher ligand loading on SBA-15 was observed in IPPL-SBA-15 1A.

#### 4.2 Application of Catalysts for CO<sub>2</sub> Hydrogenation Reaction

The catalytic efficiency of SRUCs were screened for the hydrogenation of CO<sub>2</sub> to formic acid (Table 3). The hydrogenation reaction was carried out in 100 mL autoclave with triethyl amine (NEt<sub>3</sub>) and water under the pressure of CO<sub>2</sub> and hydrogen gas (40 bar, CO<sub>2</sub>:H<sub>2</sub> = 1:1) at 75 °C. The formation of formic acid (or formate) was calculated through <sup>1</sup>H NMR spectroscopy where DMSO was used as solvent and dioxane as an internal standard (Fig. 8) [24, 27–29].

Prior to the hydrogenation reaction, the catalyst was activated by hydrogen (10 bar) for 30 min at 30 °C. The

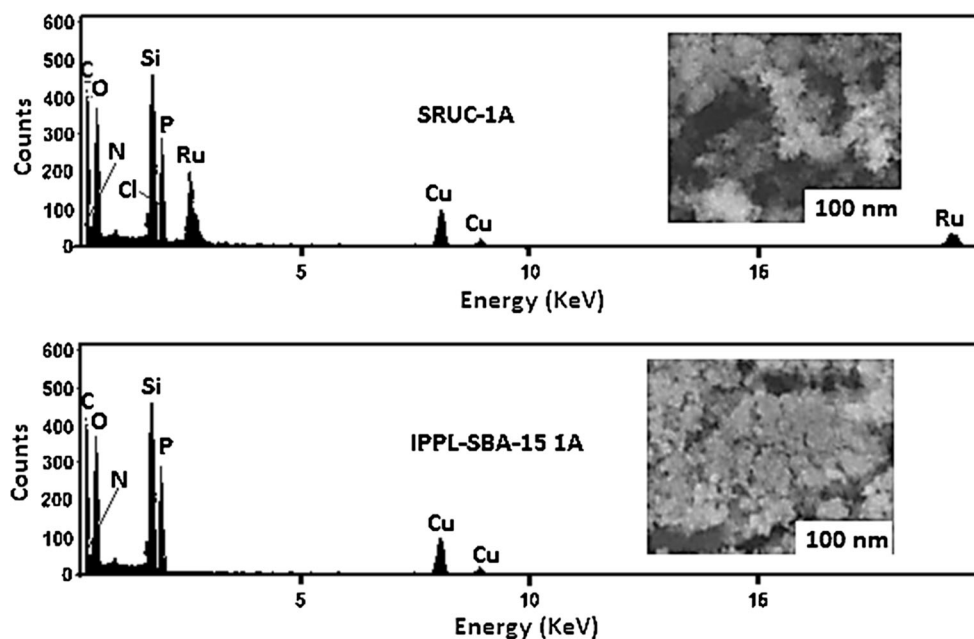


Fig. 6 SEM-EDS analysis

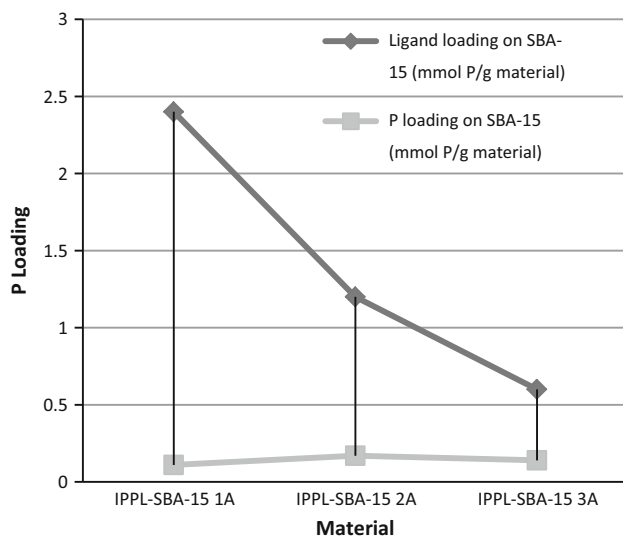


Fig. 7 Phosphine ligand (P) loading on IPPL-SBA-15 material

results obtained while utilizing the silica-tethered Ru catalysts for CO<sub>2</sub> hydrogenation were concluded in Table 3.

In the absence of a catalyst, no sign of hydrogenation reaction was observed (Table 2, Entry 1). The unsupported RuCl<sub>3</sub> precursor gave only a small amount of formic acid (Table 2, Entry 2). Even formic acid with low TON value was also attained while applying RuCl<sub>3</sub>/SBA-15 and amine-functionalized SBA-15 (**SRUC-4A**) (Table 3, entry 3) and 4). In our study it is clear that, catalytic materials with phosphine ligands gave formic acid with good TON

value (Table 3, entry 5–13). The tethered bidentate catalyst **SRUC-1A** showed high catalytic activity and we isolated formic acid with high TON value [28, 29]. After screening all the developed catalysts, we can arrange them with respect to their catalytic performance in the following order **SRUC-1A** > **SRUC-3A** > **SRUC-2A** > unsupported Ru-moiety A. The lowest catalytic performance was recorded with **SRUC-1A** mainly because of low loading of phosphine group on the support. While low activity of unsupported **Ru-moiety A** precatalyst was recorded mainly because of metal–metal dimerization in solution [24].

It is worth noted here that, tethered catalysts can be easily recovered followed by filtration. In catalyst recycling experiment of **SRUC-1A** (Fig. 9), we successfully obtained the formic acid up to nine consecutive runs. The slender drop in catalyst activity was recorded due catalyst loss during work-up, mainly because of metal leaching (observed in AAS analysis) (Fig. 10). The XPS analysis was also performed for **SRUC-1A** catalyst after the catalysis and surprisingly no changes in the binding energy of Ru 3d<sub>3/2</sub> and 3d<sub>5/2</sub> was found almost similar to the fresh **SRUC-1A** catalyst. Such observation indicates that, our catalytic system is stable in aqueous solution and for high pressure reaction condition.

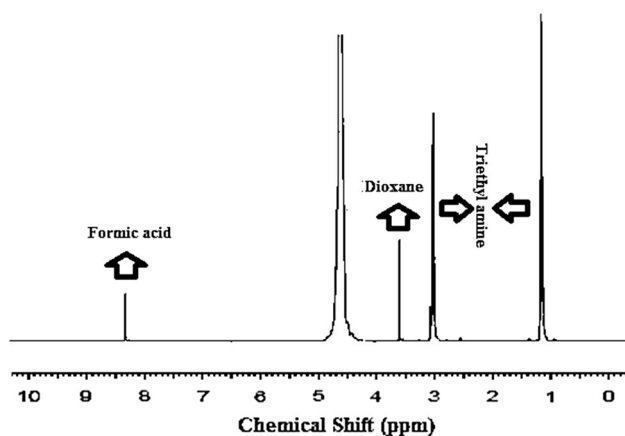
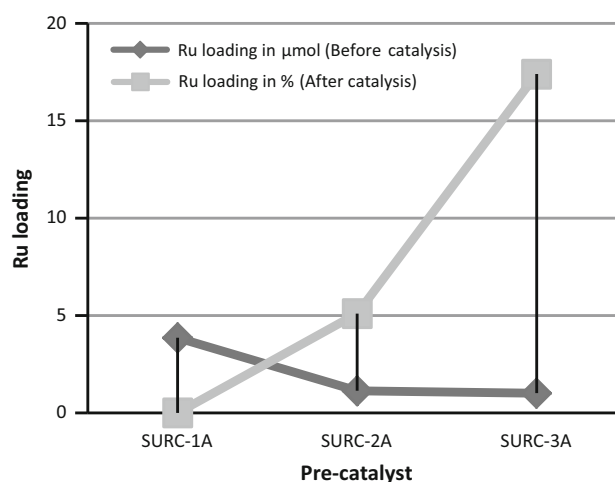
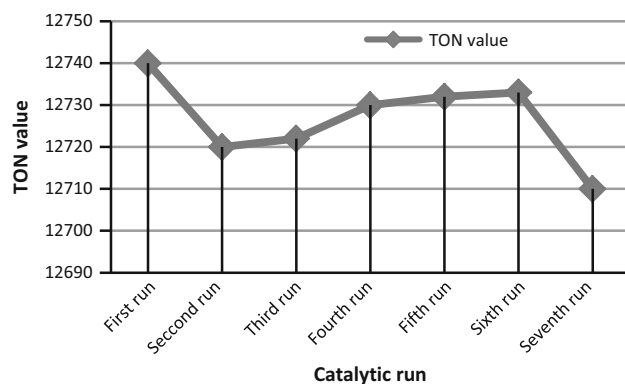
To understand the stability of the bidentate catalyst over monodentate catalyst, we performed the filtration experiment. In this experiment, at 75 °C, aqueous solution of (1 M, 5 mL) catalysts were mixed with hydrogen gas at 5 MPa for 1 h. The resulting mixture was filtered and the filtrate was used for the hydrogenation reaction. No

**Table 3** Catalyst optimization for CO<sub>2</sub> hydrogenation reaction

Entry <sup>a</sup>	Catalyst	T °C	t (h)	TON × 10 <sup>2</sup> (mol <sub>FA</sub> /mol <sub>Ru</sub> ) <sup>b</sup>	TON × 10 <sup>2</sup> (mol <sub>FA</sub> /mol <sub>Ru</sub> × h <sup>-1</sup> )
1	None	75	1	–	–
	RuCl <sub>3</sub> ·3H <sub>2</sub> O	75	1	11.1	11.1
2	RuCl <sub>3</sub> /SBA-15	75	1	18.7	18.7
3	SRUC-4A	75	1	41.6	41.6
4	SRUC-2A	75	2	67.8	33.9
5	SRUC-3A	75	2	87.1	43.55
6	SRUC-3A	75	15	96.4	6.4
7	SRUC-1A	75	1	122.7	122.7
8	SRUC-1A	75	2	143.1	71.5
9	SRUC-1A	75	15	167.2	11.1
10	SRUC-1A	100	1	131.2	131.2
11	SRUC-1A	120	2	148.9	74.4
12	Moiety-A	75	2	28.6	14.3
13	RuCl <sub>2</sub> (PPh <sub>3</sub> ) <sub>3</sub>	75	2	16.1	8.1

<sup>a</sup> Reaction condition: 100 mL (Amar autoclave) charged with double distilled water (15 mL), distilled water (15 mL), NEt<sub>3</sub> (2 mL), concentration of Ru metal in catalyst = 0.2 × 10<sup>-2</sup> g/g catalyst, total pressure 20 Bar (H<sub>2</sub>/CO<sub>2</sub> = 1:1)

<sup>b</sup> FA formic acid

**Fig. 8** <sup>1</sup>H NMR analysis for formic acid from crude reaction mass**Fig. 10** Leaching study of Ru metal in SRUC catalysts**Fig. 9** Catalytic recycling of SRUC-1A catalyst

formation of formic acid confirmed negligible catalyst leaching of active catalyst. This result was also supported by ICP-OES analysis result of filtrate where Ru metal was not detected in the solution. Monodentate catalysts gave prominent metal leaching in the solution with respect to **SRUC-1A**. It was also confirmed by ICP-OES analysis. The trend of metal leaching from highest to lowest was found in following order **SRUC-3A** > **SRUC-2A** > **SRUC-1A** (Fig. 10). Even, while performing the hydrogenation reaction using the filtrate of monodentate catalysts, we also obtained formic acid. Here we obtained the formic acid with higher TON value with **SRUC-3A** filtrate (TON = 0.8 × 10<sup>2</sup>).

## 5 Conclusion

In this manuscript, we reported a new protocol to synthesize mesoporous silica-tethered Ru complexes (**SRUC 1–4A**). Among these, materials, **SRUC 1A** was found as an effective heterogeneous catalyst for the selective CO<sub>2</sub> hydrogenation reaction to attain formic acid under normal reaction condition. In terms of catalyst recycling, this catalytic system was found highly active for 6 catalytic runs without any noteworthy loss of TON value of formic acid. In parallel, we also performed the filtration experiment and the obtained results were found in good agreement with recycling test results. Furthermore, this tethered bidentate catalyst gave high stability over the monodentate catalysts.

**Acknowledgments** This work is financially supported by DST Fast Track (SB/FT/CS-124/2012), India.

## References

1. Sedjo R, Sohngen B (2012) *Annu Rev Res Econ* 4(1):127
2. Lal R (2015) *Philos Trans R Soc B* 363(1492):815
3. Quéré CL, Raupach MR, Canadell JG, Marland G (2009) *Nat Geosci* 2(12):831
4. Richards KR, Stokes C (2004) *Clim Change* 63(1/2):1
5. Kim SH, Kim KH, Hong SH (2014) *Angew Chem Int Ed* 53(3):771
6. Cuéllar-Franca RM, Azapagic A (2015) *J CO2 Util* 9:82
7. Kondratenko EV, Mul G, Baltrusaitis J, Larrazábal GO, Pérez-Ramírez J (2013) *Energy Environ Sci* 6(11):3112
8. Gomes CDN, Jacquet O, Villiers C, Thuéry P, Ephritikhine M, Cantat T (2012) *Angew Chem Int Ed* 51(1):187
9. Lu Q, Rosen J, Zhou Y, Hutchings GS, Kimmel YC, Chen JG, Jiao F (2014) *Nat Commun* 5:1
10. Saeidia S, Amina NAS, Rahimpour (2014) *J CO2 Util* 5:66
11. Jadhava SG, Vaidyaa PD, Bhanageb BM, Joshi JB (2014) *Chem Eng Res Des* 92(11):2557
12. Hong SH (2013) *Org Chem Curr Res* 2:2
13. Gibson HW (1969) *Chem Rev* 69(5):673
14. Grasemann M, Laurency G (2012) *Energy Environ Sci* 5(8):8171
15. Johnson TC, Morrisa DJ, Wills M (2010) *Chem Soc Rev* 39(1):81
16. Laurency G, Dyson PJ (2014) *J Braz Chem Soc* 25(12):2157
17. Leitner W (1995) *Angew Chem Int Ed Engl* 34(20):2207
18. Jogunola O, Salmi T, Wärnå J, Mikkola J-P, Tirronen E (2011) *Ind Eng Chem Res* 50(1):267
19. Valkenberg MH, Holdrich WF (2002) *Catal Rev* 44:321
20. Wang W, Wang S, Maa X, Gong J (2011) *Chem Soc Rev* 40(7):3703–3727
21. Schmid L, Rohr M, Baiker A (1999) *Chem Commun* 22:2303
22. Zhang Y, Jinhua JF, Yu FY, Zheng X (2004) *Catal Lett* 93(3/4):231
23. Hicks JC, Jones CW (2006) *Langmuir* 22(6):2676
24. Xu Z, McNamara ND, Neumann GT, Schneider WF, Hicks JC (2013) *ChemCatChem* 5(7):1769
25. Ghilardi CA, Midollini S, Moneti S, Orlandini A, Scapacci G (1992) *J Chem Soc Dalton Trans* 23:3371
26. Bek D, Balcar H, Zilkova N, Zukal A, Horacek M, Cejka J (2011) *ACS Catal* 1(7):709–718
27. Behringer KD, Blumel J (1996) *Inorg Chem* 35(7):1814
28. Srivastava V (2014) *Catal Lett* 144(10):1745
29. Srivastava V (2014) *Catal Lett* 144(12):2221